

Saline Aquifer CO₂ Storage Project, SACS, Phase II

Task 3.2: Geochemical laboratory experiments

Mineralogical and petrophysical properties of
Utsira sand before and after reaction with
CO₂ saturated formation water

Niels Springer, Christian Høier and Holger Lindgren

Confidential report

Copy No.

Not to be released

Summary

This report collects the work carried out at the Geological Survey of Denmark and Greenland (GEUS) under the international Saline Aquifer CO₂ Storage (SACS) project. The aim of the project has been to study the effect of CO₂ sequestration in the Utsira sand aquifer in the Sleipner area, the Norwegian North Sea, by conducting laboratory experiments and modelling scenarios to predict any long term effects.

GEUS Core Laboratory has undertaken analysis of core material from the Utsira sand to characterize mineralogical and petrophysical properties before and after reaction with supercritical CO₂-saturated formation water. This work formed part of the "Task 3.2: Geochemical laboratory experiments" to help determine baseline conditions for the modelling work. Most experiments were performed as short term (2-4 weeks) dynamic flooding tests at overburden or reservoir conditions, 100 bar (1450 psi) net effective stress, 100 bar (1450 psi) pore pressure and 37 °C.

The mineralogical study showed a significant drop in sample surface area after test due to dissolution of carbonate shells in the sand. A special study with AFM (atomic force microscope) did not reveal any dissolution-precipitation processes taking place for the main minerals quartz and mica in the Utsira sand when subjected to reaction with CO₂-saturated formation brine. Cation exchange capacity remained unchanged for the CO₂ reacted samples.

Unconfined room condition measurements of preserved samples from a 0.9 meter deep frozen core section showed a mean porosity of 41.5% for the Utsira sand. When confining pressure equal to ~900 meter TVD is applied to the samples the porosity is reduced to approx. 38-39%. This is the depth from which the present core was cut. A best estimate of the porosity reduction and pore volume compressibility was obtained. It was observed that unconsolidated samples do not keep a solid form during overburden experiments. Water acts as a lubricant and even long time after confining pressure has been posed on the sample, grains re-arrange which means small changes in bulk and pore volume. Thus small changes in volume due to dissolution of minerals by CO₂ saturated water cannot be discriminated from grain re-arrangement in tests of unconsolidated sediments. Packing of the sand and fines migration is by far the most important phenomena affecting the measured permeability, even overshadowing the effect of confining pressure. After repeated testing of many samples it was found that the gas and Klinkenberg corrected gas permeability for the tested Utsira sand core section is within the range 1.5-2.5 D. The liquid permeability is lower at 1-1.5 D, mainly due to fines migration. In the CO₂ reaction experiments Ca seems to be the most reactive element due to solution of carbonate shell fragments in the sand.

Contents

SUMMARY	1
1 INTRODUCTION	3
2 SAMPLING AND ANALYTICAL PROCEDURE	4
2.1 FLOW CHART OF THE ANALYTICAL PROCEDURE	5
3 MINERALOGY	6
3.1 METHODS	6
3.2 RESULTS	7
4 POROSITY	10
4.1 POROSITY OF PRESERVED SAMPLES	10
4.2 POROSITY AT OVERBURDEN PRESSURE	10
4.3 POROSITY REDUCTION AND COMPRESSIBILITY	11
4.4 POROSITY CONCLUSIONS	11
5 PERMEABILITY	17
5.1 PHYSICAL CONDITIONS FOR THE UTSIRA SAND AT SLEIPNER	17
5.2 FORMATION WATER COMPOSITION	17
5.3 GAS AND LIQUID PERMEABILITY AT OVERBURDEN PRESSURE	18
5.4 DYNAMIC CO ₂ FLOODING EXPERIMENTS	20
5.5 PERMEABILITY CONCLUSIONS	20
6 ANALYTICAL METHODS	24
6.1 CONVENTIONAL CLEANING AND DRYING	24
6.2 GAS PERMEABILITY (GEUS STEADY STATE INSTRUMENT)	24
6.3 KLINKENBERG PERMEABILITY (GEUS STEADY STATE INSTRUMENT)	24
6.4 LIQUID PERMEABILITY	24
6.5 HE-POROSITY AND GRAIN DENSITY	24
6.7 REDUCED POROSITY BY OVERBURDEN PRESSURE	25
6.8 PORE VOLUME COMPRESSIBILITY	25
6.9 PRECISION OF ANALYTICAL DATA	26
6.10 NOMENCLATURE	26
7 REFERENCES	27

Req. no.: 09213-474
Files: Sacsrep1.doc

1 Introduction

As a partner in the Saline Aquifer CO₂ Storage (SACS) project, GEUS Core Laboratory has participated in subtasks 1.5 "Evaluation of Formation Fluids" and 3.2 "Geochemical Laboratory Experiments". GEUS obligation have been to analyze core samples of the Utsira Formation to deliver the necessary laboratory information needed for the subtask work. This report present the results obtained from task 3.2 on unconsolidated sand from the Neogene Utsira Sand unit in the Viking Graben, the Norwegian North Sea. The analytical programme involved the following characterization:

- Mineralogy before and after reaction with CO₂ -saturated formation water
- Surface properties before and after reaction with CO₂ -saturated formation water
- Porosity measurements on sandpacks and frozen samples
- Porosity at overburden pressure and pore volume compressibility
- Gas and liquid permeability at overburden pressure
- Short term CO₂ flooding experiments

Several Technical Reports with core data have been issued to the SACS partners during the project period. This report collects all data and results of the analytical programme.

2 Sampling and analytical procedure

On March 17, 1999 GEUS Core Laboratory received 5 pieces of frozen 4" diameter core, in total 0.9 meter core covering the interval 1084.1 – 1085.0 meter MD from the well 15/9-A23 in the Sleipner field, Norwegian North Sea. The core pieces were delivered by courier from ResLab A/S in Stavanger, contained in a freeze box and preserved in ordinary plastic bags but appeared to be in a good condition.

Immediately 4 plug samples ($\varnothing \sim 38$ mm) were drilled using dry nitrogen gas as a coolant. These plugs were used for formation water analysis (Subtask 1.5) but also supplied routine core analysis data after formation water had been extracted by centrifuging. An additional number of preserved plugs were taken from the frozen core and kept for later dynamic flooding experiments, fig. 2.1. Finally the core was described and a number of small samples taken for petrographical characterization (Work Area 1: Geology). Later, the core pieces were allowed to thaw, and both uncleaned and cleaned material were used for testing.

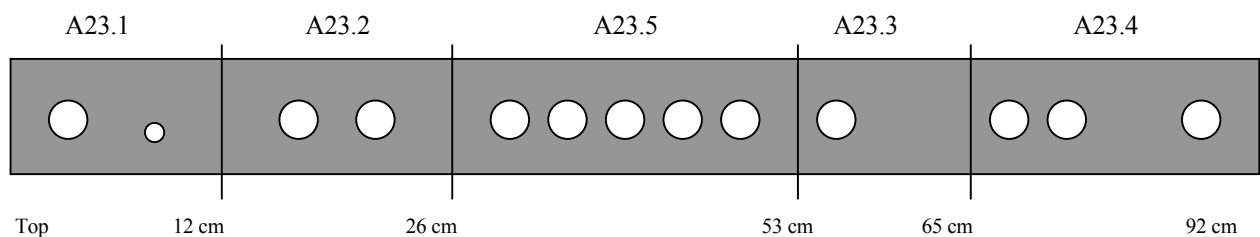


Figure 2.1: Sleipner 15/9-A23. Sketch showing the 5 frozen core sections received for SACS Task 1.5 and 3.2. Total length is approx. 0.9 meter. Approximate sampling positions are indicated.

From inspection of plug trims and material left from the 4 plugs drilled for formation water analysis, the Utsira sand from this core section appear as a grey unconsolidated fine to medium grained, poorly sorted sand. Grains are angular to subangular. The plugs used for formation water extraction and core analysis were later used for mineralogical analysis. The analytical procedure applied to both uncleaned and cleaned core material is shown in section 2.1.

3 Mineralogy

The objective has been to characterize the mineralogical composition of the core section from the 15/9-A23 well to be used during dynamic flooding experiments in the geochemical study. If possible, mineral-surface reactions after brine-CO₂ flooding should be described.

3.1 Methods

Four core plugs, A23.1 - 23.4, were originally drilled from the 1 meter of frozen core and used for extraction of pore water. After centrifugation, the loose sand from the plugs were cleaned in methanol, dried and analyzed at GEUS Clay Minerals Lab. The following parameters were determined, ref. Table 3.1:

- 1) Bulk mineralogy, qualitatively. Based on this investigation, additional quantitative analyses were made:
- 2) Determination of proportion of clay (<2 μm) and semi-quantitative determination of clay mineralogy
- 3) Semi-quantitative determination of proportion of muscovite in bulk sample
- 4) Quantitative determination of amount of quartz
- 5) SEM/EDX typing of feldspar in sample A.23.3
- 6) Determination of specific surface area
- 7) Determination of amount of CaCO₃
- 8) Determination of cation exchange capacity (CEC)

Bulk XRD mineralogical analysis. Samples were hand-ground to pass a 0.25mm sieve and X-ray diffraction carried out using a Philips 1050 instrument and Co-K α radiation on randomly oriented specimens.

Determination of proportion of clay (<2 μm). The samples were split into grain size fractions >2 μm and <2μm in a particle size centrifuge. The fractions were weighed after air-drying. The clay mineralogy was determined semi-quantitatively for all samples by X-ray diffraction (Co-radiation) on oriented specimens of clay fractions saturated with specific cations and with/without glycerol.

Semi-quantitative determination of proportion of muscovite in bulk sample. The amount of muscovite was estimated by X-ray diffraction on randomly oriented specimens using a muscovite from Iveland, Norway, (hand-ground to <0.25 mm size) as external standard.

Quantitative determination of amount of quartz. The amount of quartz was determined by X-ray diffraction on randomly oriented specimens using quartz 4.5-45 μm as external standard. Because of the larger grain size of the samples, the samples were ground to pass a 63 μm sieve before analysis.

SEM/EDX typing of feldspar. Performed on a slide of Utsira sand by EDX element image analysis in the SEM instrument.

Determination of specific surface area. The specific surface area was determined by the BET method using nitrogen as adsorbent at liquid nitrogen temperature. The instrument was a Micromeritics Accusorb.

Determination of amount of CaCO₃. The amount of CaCO₃ was determined by differential thermal analysis (DTA) with infrared spectrometric determination of evolved gases CO₂, H₂O and SO₂. By this method, down to 0.1% of carbonates can be determined accurately.

Determination of CEC. Cation exchange capacity (CEC) was determined by exchange with sodium at pH 8.2, washing out of excess sodium chloride and exchange of sodium by ammonium. Exchanged sodium was determined by atomic absorption spectrometry.

3.2 Results

Unreacted samples. All samples had a very high content of quartz (69-91%) with minor amounts of feldspar and mica, table 3.1. In addition, shell fragments was seen in all samples and small amounts of kaolinite could be detected in A23.1. The clay fraction consisted of approximately equal amounts of kaolinite, illite and smectite; quartz was present as well.

Table 3.1 Summary of the mineralogical analysis of Utsira sand from well 15/9-A23. Samples are taken within a core section of 0.9 meter (1084.1-1085.0).

Mineralogy of bulk samples:								
Plug No.	Depth	Bulk (1)	Clay (2)	Mica (3)	Quartz (4)	Feldspar (5)	S _{BET} (6)	CaCO ₃ (7)
	meter	mineralogy	%	%	%	%	m ² /g	%
A-23.1	1084,13	quartz, mica & feldspar (minor)	0,9	5-10	80	n.d.	0,3	2.1
A-23.2	1084,28		0,5	<5	88	n.d.	0,2	3.7
A-23.3	1084,65		0,8	<5	69	5-10	0,4	2.7
A-23.4	1084,94		1,5	<5	91	n.d.	0,3	2.3

Reacted samples. Two reacted samples were deep frozen after completion of the CO₂-flooding experiment and then cut into 2-3 pieces determined for mineralogical analysis, table 3.2. The specific surface area and cation exchange capacity (CEC) was compared with an unreacted reference sample. The surface area is significantly lower in the reacted samples, probably because of dissolution of carbonate shells during CO₂-flooding; no change in CEC was obvious presumably because no reaction occurred in the clay fraction. Material intended for XRD identification was crushed to pass a 250 µm sieve and diffractograms recorded for all sample pieces. A difference between the unreacted and the reacted Utsira sand could not be detected.

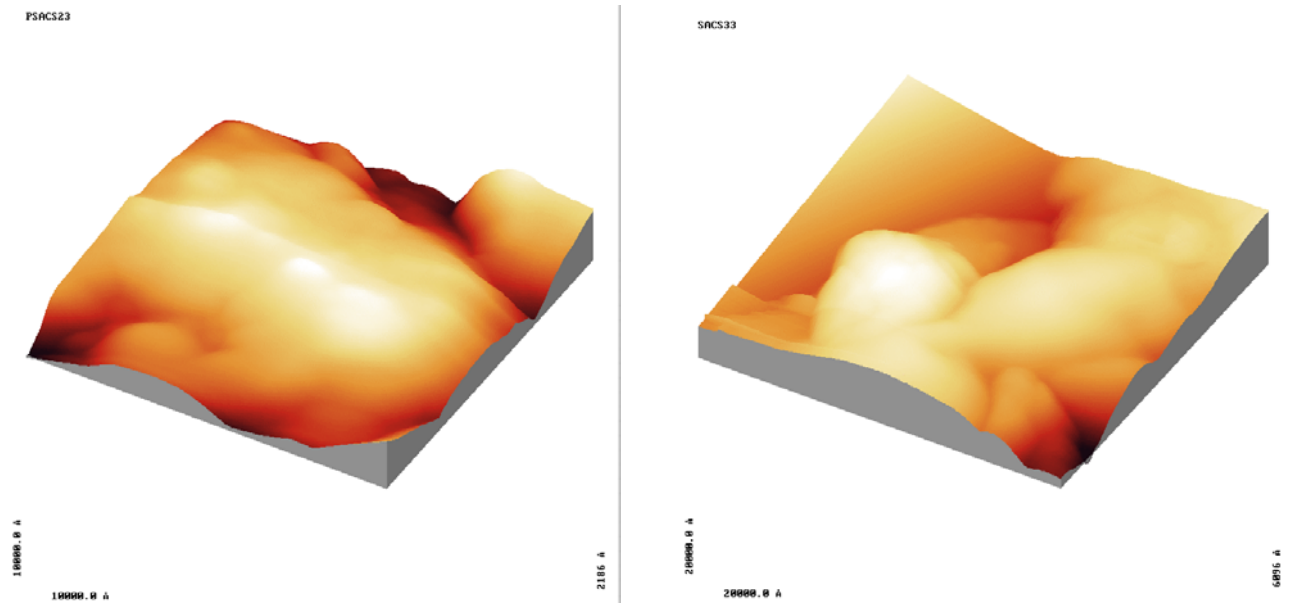
Atomic Force Microscopy (AFM) observations. From unreacted and reacted samples material have been investigated for surface dissolution/precipitation processes by AFM. The samples were suspended by ultrasonic treatment in distilled water and a drop containing the finer particles was left to dry on a block of highly oriented pyrolytic graphite. The specimen were scanned in non-contact mode at atmospheric conditions (humidity and temperature). A large number of scans (~50) were carried out for each sample specimen. Final images were prepared for two different particles from each sample, one type being a sheet type, probably mica, and another being a blocky quartz. However, it was not possible to observe any surface changes due to reaction with CO₂-saturated formation brine in any of the images produced, fig. 3.1. Dissolution/precipitation processes in the Utsira sand due to reaction with CO₂-saturated formation water is expected to produce surface effectes (etch holes, newformation) with a habit characteristic of the crystal symmetry system for the subject mineral (e.g. quartz: trigonal or pseudo hexagonal structures)

Table 3.2. *Accusorp determinations on reacted Utsira sand show significantly lower surface areas than the unreacted samples and the reference sample. CO₂-reacion experiment performed at reservoir temperature for a period of 2-4 weeks.*

Properties of bulk samples:					
Plug No.	Depth meter	Clay %	S_{BET} m²/g	CEC meq. Na⁺/100 g	Comment
A-23.1	1084.13	0.9	0.3		Un-reacted samples
A-23.2	1084.28	0.5	0.2		
A-23.3	1084.65	0.8	0.4		
A-23.4	1084.94	1.5	0.3		
A-23.4 B	1084.97		0.3	220	
A-23.6 B	1084.51		0.3	220	
A-23.7	1084.71				
Reference sample			0.5	240	
A 23.5 upstream end	1084.46		0.1	250	Reacted sample (14 days)
downstream end			0.1	250	
A 23.6 upstream end	1084.51		0.2	250	Reacted sample (31 days)
central part			0.2	240	
downstream end		0.2 *	0.1	230	

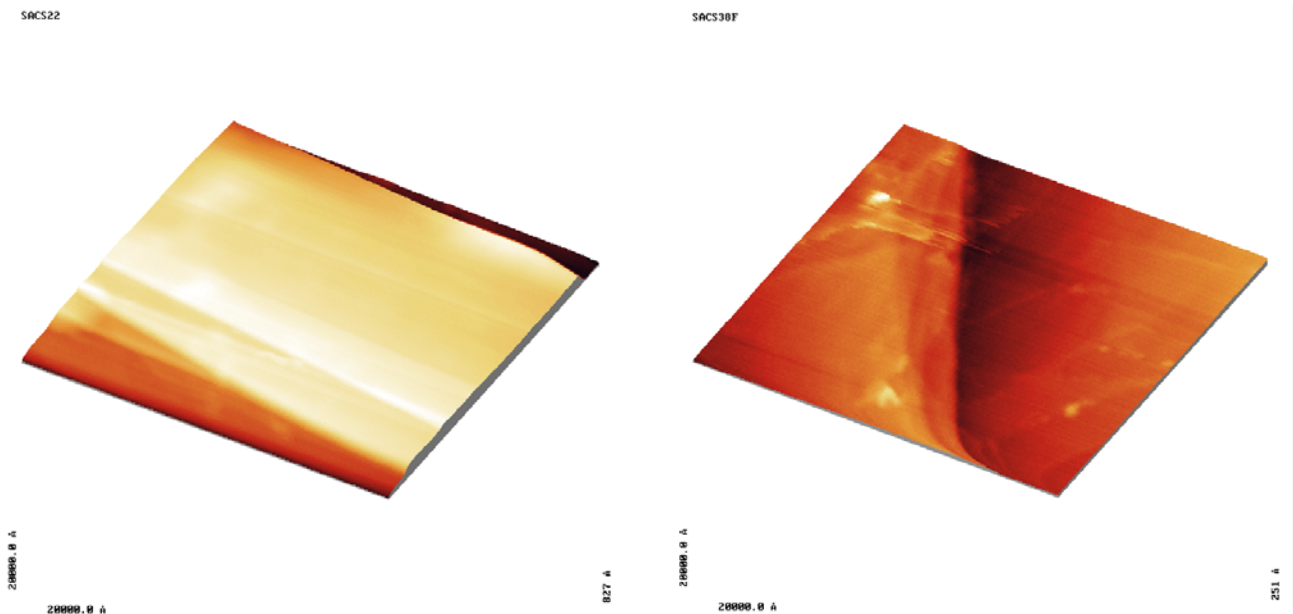
* The clay fraction from this reacted sample contains quartz, smectite, illite and traces of chlorite.

Fig. 3.1. Rasterscope 3D AFM-images of selected grains from unreacted and CO₂-reacted Utsira sand samples. The specimen were scanned in non-contact mode at atmospheric conditions (humidity and temperature). Each surface scan represent 256x256 points. Width and height of the image is given in Ångström (E-10 meter).



A23.2, reference sample, showing surface of a quartz grain from an unreacted Utsira sand.

A23.6, surface of a quartz grain from a reacted Utsira sand after 31 days.



A23.2, reference sample, showing surface of a layer silicate from an unreacted Utsira sand.

A23.6, surface of a layer silicate from a reacted Utsira sand after 31 days (left hand side of image, to the right is the graphite substrate).

4 Porosity

During the study the porosity of the Utsira sand was determined on both preserved (frozen) and cleaned (loose sand) samples dependant on the experimental conditions.

4.1 Porosity of preserved samples.

The bulk volume of a frozen plug was calculated from calliper dimensions. After dynamic testing the sample was soxhlet cleaned and dried at 60 °C. The unconsolidated sand was now quantitatively transferred to a measuring cup and the grain volume determined using the He-expansion technique. The pore volume then appears as the difference between the bulk volume and the grain volume, table 4.1.

4.2 Porosity at overburden pressure

The porosity at overburden conditions was determined by different techniques depending on the experimental design:

- A cleaned, dried and weighed sample of loose sand was placed in a hydrostatic core holder and the confining pressure increased to 100 bar. The sample pore volume was determined by the He-expansion technique in a Boyle's law single cell configuration for direct pore volume measurement. The sample grain volume was calculated from an estimated grain density of 2.66 g/cc, table 4.1.
- In dynamic flow tests using preserved (uncleaned) sand and simulated formation brine, the initial sample porosity is set at 41.5%. This is based on porosity measurement of cleaned and dried sand in a sample cup connected to the Helium porosimeter operated at room conditions. The frozen plug or uncleaned sand is then packed in a core holder or long core holder at 10 bar confining pressure and fully saturated with simulated formation brine by flooding several pore volumes of brine through the sample. In time steps of one hour the confining pressure was raised to 30, 50, 70 and 100 bar, and the produced brine was monitored by an electronic balance. The sample pore volume reduction and compressibility was calculated from the recorded production data, section 4.3 below.

Table 4.1. The table below shows the porosity measured at the frozen plugs at room conditions and at unconsolidated cleaned sand measured at overburden pressure.

Sample ID	Preserved (frozen) plug				Cleaned sand @100 bar confining pressure			
	BV cc	DW g	Porosity %	Grain density g/ml	BV cc	DW g	Porosity %	Grain density g/ml
A23.1	53.62	82.10	42.45	2.661	31.78	54.4	35.8	2.66*
A23.1			-	-	32.44	55.0	36.2	2.66*
A23.2	52.68	81.40	41.85	2.657			-	-
A23.3	52.42	82.40	40.71	2.651	32.06	55.0	35.5	2.66*
A23.4	52.96	83.80	40.47	2.658			-	-
A23.5			-	-	29.21	50.0	35.7	2.66*
A23.5			-	-	32.68	55.0	36.7	2.66*

*Assumed grain density

4.3 Porosity reduction and compressibility

The experimental procedure applied during the dynamic flooding runs allowed a determination of the pore volume compressibility and porosity reduction as a function of confining pressure. The table below shows the measured brine production as a function of the increasing pressure. A line is fitted and measured brine is corrected with respect to mass and volume. The corrected data is used to calculate porosity reduction and pore volume compressibility. Two slightly different types of experiments were conducted. Preserved plugs (frozen), later used for CO₂ flooding experiments, were measured for porosity reduction during the general laboratory testing procedure, table 4.2 – 4.4. Long core sand packs, primarily meant for precise measurement of liquid permeability, were measured for porosity reduction as well, table 4.5 – 4.6.

4.4 Porosity conclusions

After retrieval from the core barrel the unconsolidated Utsira sand was preserved by deep freezing. The core may easily have been reworked downhole during the coring action, and the freezing technique is therefore by no means a guarantee that the original texture of the sand was preserved. From unconfined room condition measurements of frozen plug samples, table 4.1, the mean porosity of the sand is 41.5%. Data measured for sand packs at 100 bar confining pressure gives porosity values in the range 35.5-36.7%. Considering the pore volume compressibility data, it is reasonable to conclude that the reservoir porosity in ~900 meter TVD (equal to 70 bar hydrostatic confining pressure) is 38-39%. This is the depth from which the present core was cut. A best estimate of the porosity reduction and compressibility is given in the table below.

It was observed that unconsolidated samples do not keep a solid form during overburden experiments. Water acts as a lubricant and even long time after confining pressure has been posed on the sample, grains rearrange which means small changes in bulk and pore volume. Thus small changes in volume due to dissolution of minerals by CO₂ saturated water cannot be discriminated from grain re-arrangement in tests of unconsolidated sediments.

Table 4.7. *Average porosity reduction and pore volume compressibility for a 41.5% porosity Utsira sand from the 15/9-A23 well. Best estimate data from tables 4.2-4.6 below.*

Pressure bar	Pressure psi	Porosity %	Reduction %	Compressibility vol/vol*psi
0	0	41.5	100.0	-
10	145	40.9	98.6	1.47E-04
30	435	40.1	96.6	1.00E-04
50	725	39.5	95.2	7.50E-05
70	1015	39.0	94.0	6.01E-05
100	1450	38.9	93.7	5.74E-05

Table 4.2. Pore volume reduction and compressibility for preserved sample A23.5.

Pressure bar	Pressure psi	Corrected g	Corrected ml	BV ml	GV ml	PV ml	Porosity %	Reduction %	Compress. vol/vol*psi
0	0	0.00	0.00	87.81	51.37	36.44	41.50	100.00	
10	145	0.72	0.71	87.10	51.37	35.73	41.02	98.86	1.26E-04
19	276	1.23	1.21	86.60	51.37	35.23	40.68	98.04	1.17E-04
37	537	2.30	2.25	85.56	51.37	34.19	39.96	96.30	9.82E-05
62	899	3.32	3.25	84.56	51.37	33.19	39.25	94.59	6.95E-05

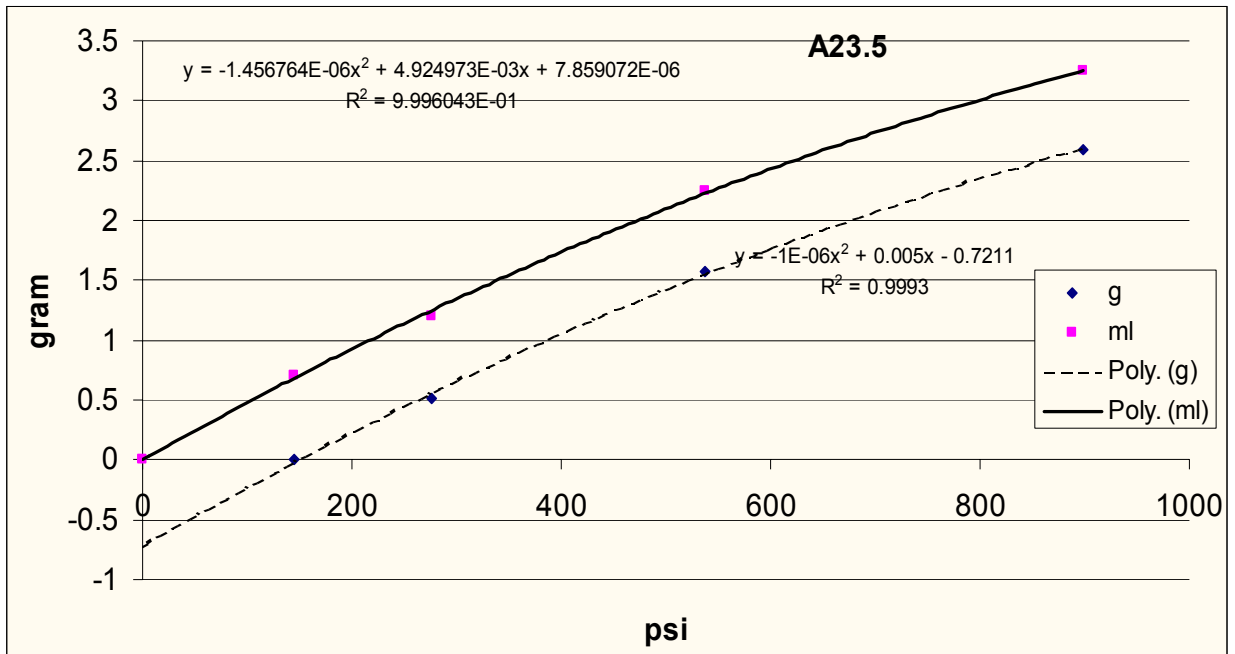


Figure 4.2: Extrapolation of water production between 0 – 10 bar, and the corrected brine production curve for sample A23.5.

Table 4.3. Pore volume reduction and compressibility for preserved sample A23.6.

Pressure bar	Pressure psi	Corrected g	Corrected ml	BV ml	GV ml	PV ml	Porosity %	Reduction %	Compress. vol/vol*psi
0	0	0.00	0.00	81.78	47.84	33.94	41.50	100.00	
10	145	0.63	0.62	81.16	47.84	33.32	41.06	98.93	1.15E-04
19	276	1.10	1.07	80.71	47.84	32.87	40.72	98.13	9.67E-05
37	537	1.82	1.78	80.00	47.84	32.16	40.20	96.87	7.18E-05
62	899	2.59	2.53	79.25	47.84	31.41	39.63	95.50	6.49E-05

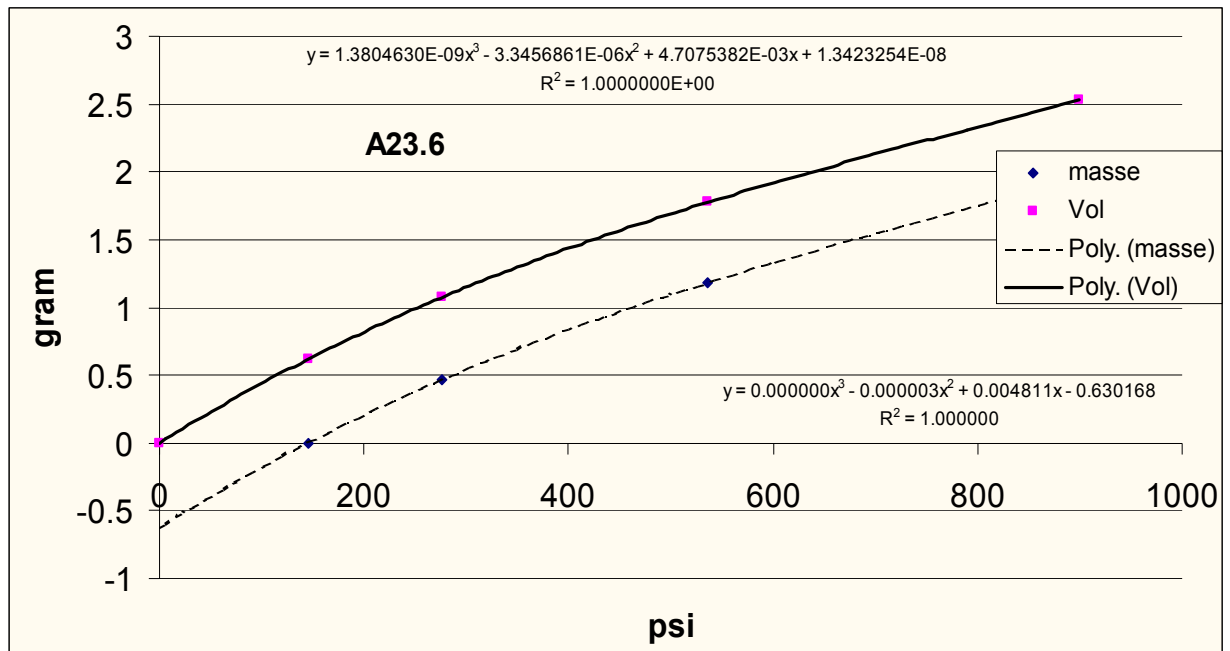


Figure 4.3: Extrapolation of water production between 0 – 10 bar, and the corrected brine production curve for sample A23.6.

Table 4.4. Pore volume reduction and compressibility for preserved sample A23.7.

Pressure bar	Pressure psi	Corrected g	Corrected ml	BV ml	GV ml	PV ml	Porosity %	Reduction %	Compres. vol/vol*psi
0	0	0.00	0.00	90.69	53.05	37.64	41.50	100.00	
10	145	0.75	0.73	89.96	53.05	36.91	41.03	98.85	1.17E-04
19	276	1.13	1.10	89.59	53.05	36.53	40.78	98.26	1.02E-04
37	537	2.11	2.07	88.62	53.05	35.57	40.14	96.71	6.95E-05
62	899	2.64	2.59	88.10	53.05	35.05	39.79	95.86	2.17E-05

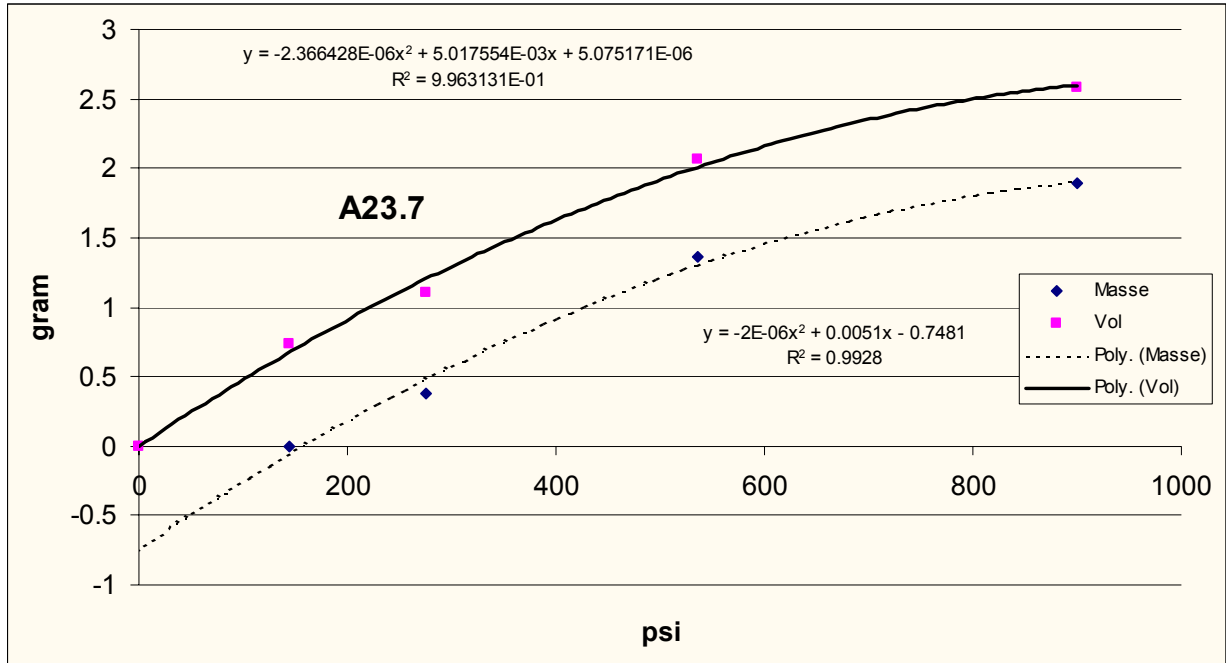


Figure 4.4: Extrapolation of water production between 0 – 10 bar, and the corrected brine production curve for sample A23.7.

Table 4.5. Pore volume reduction and compressibility for long core sample A23.1L.

Pressure bar	Measured g	Corrected g	Corrected ml	BV ml	GV ml	PV ml	Porosity %	Reduction %	Compres. vol/vol*psi
0	-	0.0	0.0	211.01	123.44	87.57	41.50	100.00	-
10	0.0	3.4	3.3	207.67	123.44	84.23	40.56	97.74	2.37E-04
30	4.6	8.0	7.9	203.15	123.44	79.71	39.24	94.54	1.54E-04
50	7.7	11.1	10.9	200.10	123.44	76.66	38.31	92.32	1.22E-04
70	10.4	13.8	13.5	197.52	123.44	74.08	37.50	90.37	1.17E-04
100	13.9	17.3	17.0	194.05	123.44	70.61	36.39	87.68	9.21E-05

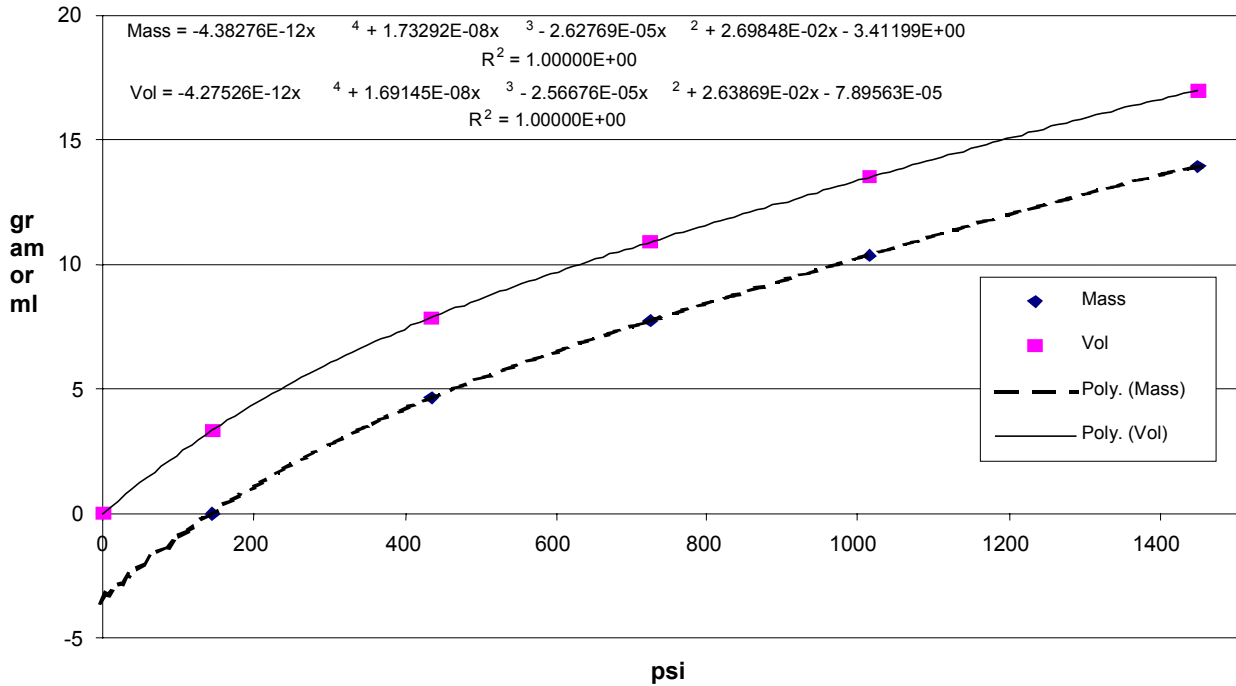


Figure 4.5: Extrapolation of water production between 0 – 10 bar, and the corrected brine production curve for sample A23.1L.

Table 4.6. Pore volume reduction and compressibility for long core sample A23.5L.

Pressure bar	Measured g	Corrected g	Corrected ml	BV ml	GV ml	PV ml	Porosity %	Reduction %	Compres. vol/vol*psi
0	0.0	0.0	0.0	213.3	124.7	88.6	41.5	100.0	-
10	0.0	2.1	2.1	211.2	124.7	86.5	40.9	98.6	1.39E-04
30	2.6	4.8	4.7	208.6	124.7	83.9	40.2	96.9	7.75E-05
50	4.2	6.3	6.2	207.1	124.7	82.3	39.8	95.8	5.70E-05
70	5.6	7.7	7.5	205.8	124.7	81.0	39.4	94.9	5.41E-05
100	7.1	9.3	9.1	204.2	124.7	79.5	38.9	93.7	2.27E-05

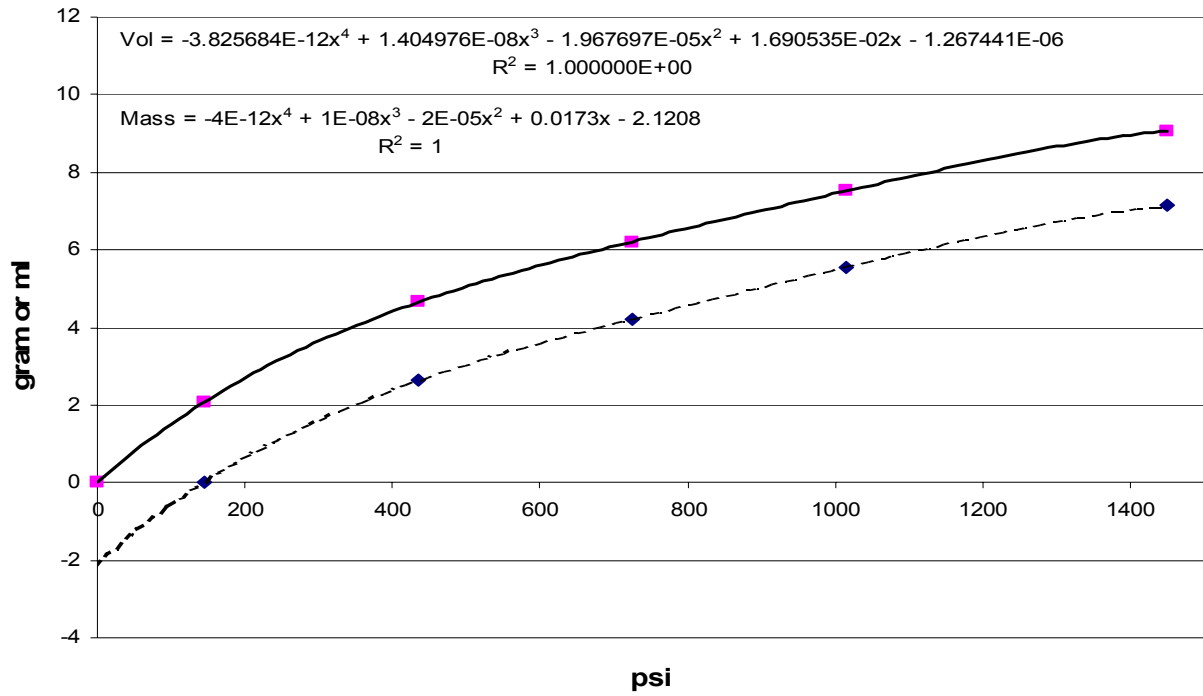


Figure 4.6: Extrapolation of water production between 0 – 10 bar, and the corrected brine production curve for sample A23.5L.

5 Permeability

The objective of the CO₂ -flooding experiments has been to study the effect on porosity and permeability and detect mineralogical reactions. CO₂-saturated formation brine was flooded through the samples at reservoir conditions at low flow rates for periods of one to four weeks duration. Liquid fractions were collected and analyzed, and after test the samples were mineralogical analyzed to detect any reactions, ref. section 3 of this report.

5.1 Physical conditions for the Utsira sand at Sleipner

The reservoir properties for the Utsira sand were mainly taken from the Phase I report (SACS, 2000).

Table 5.1. *Physical conditions for the Utsira reservoir in the Sleipner area. The core section delivered to GEUS originates from the 15/9-A23 well.*

Property	Value/range
Top Utsira sand, TVD _{ss}	854 meter
GEUS core section, TVD _{ss}	~909 meter
Reservoir pressure, top	107 bar
Reservoir temperature	37 °C
Reservoir permeability, liquid	~1 D (range 1-8 D)
Reservoir porosity, log	30-40 %
Sand thickness	150-250 meter

Based on these data it was decided to run the reservoir condition experiments at least up to a net confining pressure of 70 bar, some experiments were taken to 100 bar as well; pore pressure was set at 100 bar. Data for overburden porosity have already been presented in section 4.

5.2 Formation water composition

No information on the formation water composition in the Sleipner area was available, and water extracted from preserved plugs in Task 1.5 was heavily contaminated with drilling fluids. It was then decided to use data from the Oseberg Field, table 5.2.

Table 5.2. *Chemical composition and physical properties of the simulated formation water used in the present study. Data originates from the SACS Phase 0 report (1998), except density and viscosity data that was measured by GEUS Core Laboratory.*

Element	Concentration mg/l
Na total	10392
K+	208
Mg ²⁺	630
Ca ²⁺	426
Sr ²⁺	10
Ba ²⁺	1
Cl ⁻	18482
HCO ₃ ⁻	707
TDS:	30856
Density:	1.018 g/ml @ 22°C
	1.012 g/ml @ 37°C
	1.004 g/ml @ 70°C
Viscosity:	0.98 cP @ 22°C
	0.71 cP @ 37°C
	0.43 cP @ 70°C

5.3 Gas and liquid permeability at overburden pressure

It should be observed that the unconsolidated core material recovered from the A23 well has never been subject to routine core analysis. In addition to the porosity measurements it was therefore decided to run a number of routine gas permeability measurements before the dynamic flooding experiments started.

The permeability at overburden conditions was determined by different techniques depending on the experimental design:

- The unconsolidated cleaned and dried sand was packed in a long core holder (~½ meter) at a reduced sample diameter (2.5 cm) to overcome the problem with the uncertain determination of the liquid permeability at low flow rates. The confining pressure was slowly raised to 100 bar. The conventional and Klinkenberg corrected gas permeability was measured at room temperature. In some cases the liquid permeability was measured afterwards.
- The unconsolidated dried sand was packed in a core holder and the confining pressure was slowly raised to 100 bar. The sample was flow saturated with simulated formation brine using a slight back pressure and the liquid permeability was measured at reservoir temperature (37 °C).
- A number of experiments were carried out as blind runs and CO₂ reaction runs at reservoir conditions i.e. 100 bar pore pressure and 37 °C temperature. A constant liquid flow rate was applied, and the liquid permeability was logged continuously. Data was uncertain in most experiments due to the small differential pressure across the short samples and the low flow rates applied in the reaction experiments. A sketch of the reservoir condition flooding rig is shown below.

Data for gas and liquid permeability are shown in table 5.3 below. Because preserved samples were used for the CO₂ reaction runs, gas permeability was measured on a number of uncleaned samples to obtain as much information as possible from the limited volume of core material. Uncleaned Utsira sand has a slightly higher porosity than cleaned sand, which could increase the measured gas permeabilities. However, as appears from the table, the different grain packing and variation in particle size between the different sand packs seems to have a much more pronounced effect on the measured permeability. Sometimes a fair reproducibility can be obtained as demonstrated by sample A23.1L and A23.1L repacked. Also reversing the flow gave reproducible results for sample A23.3L. The Klinkenberg corrected gas permeability measurements are more scattered than is seen for consolidated samples. This is reflected in the Klinkenberg value sometimes being larger than the routine gas permeability value.

By far the most serious problem in permeability measurement was fines migration (Priisholm et al., 1987). Fines in general have only a small effect on gas permeability because fines tend to stick on pore surfaces when the rock is dry. As soon as the sample is saturated with a liquid, the fines get mobilized from the surface and is ready to migrate with the fluid flow through the porous network. Fines may originate from within the sediment itself or they are generated during the drilling/coring process, e.g. as fines from the drilling mud. Another challenge was loose sand grains moving into the core holder inlet and outlet tubing in response to increasing confining pressure and flow. This was prevented by inserting Ni-coated bronze filter plates of 80 µm mean pore size at each end of the sample. These filter plates was found not to restrict the measurement of permeability, but could not prevent fines migration, whereby fine grained material are slowly carried away from the sample with the flowing liquid phase. Fines may still affect the measured permeability because they tend to block pore necks within the sample and thereby restrict fluid flow. In the experiments this is seen as a dropping permeability as a function of time and can be very significant. An example, though not very serious, is seen from table 5.3 for samples A23.3L and A23.5L. The data listed represent liquid permeability measurements taken on the same sandpack during a period of several hours. It is observed that the liquid permeability decreases 5-10% due to fines migration. Re-arrangement of single grains in response to the confining pressure may contribute as well.

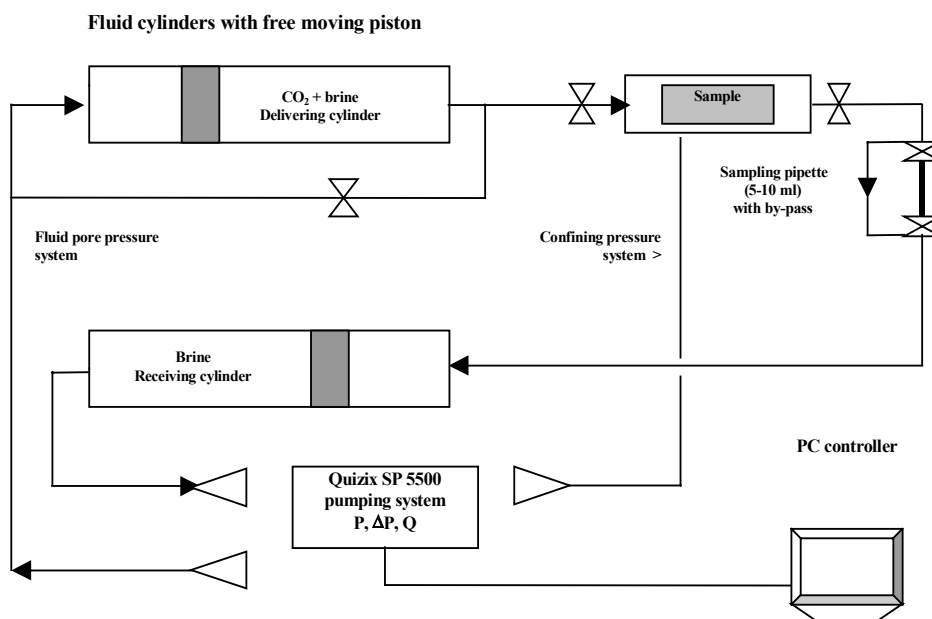
Table 5.3. *Utsira sand permeability measured at room temperature or reservoir temperature (liquid permeability) on cleaned and uncleaned samples.*

Sample	Preserved samples @ 100 bar confining pressure			Cleaned samples @ 100 bar confining pressure		
	Gas perm mD	Klink perm mD	Liquid perm mD	Gas perm mD	Klink perm mD	Liquid perm mD
A23.1L*	2293	-	774	-	-	-
	2312	-	902	-	-	-
	2322	-	-	-	-	-
	2298	-	-	-	-	-
	2400	2407	-	-	-	-
	2421	-	-	-	-	-
	2431	-	-	-	-	-
A23.1L* (repacked)	2321	2300	860	-	-	-
	-	-	884	-	-	-
	-	-	851	-	-	-
	2406	-	-	-	-	-
	2430	-	-	-	-	-
A23.3L*	1865	1859	1247	1591	1635	1213
	1844	-	1197	1553 ¹	1523 ¹	1231 ¹
	1877	-	-	1591 ²	1636 ²	1244 ²
	1842	-	-	1597 ¹	1577 ¹	1185 ¹
	-	-	1168	1589 ²	1497 ²	1246 ²
	-	-	-	-	-	-
A23.5L*	-	-	1710	986	967	582
	-	-	1625	954	-	558
	-	-	1539	-	-	-

* Long core sample, L ~ 41-43 cm, D ~ 2.5 cm

1 – first flow direction 2 – reverse flow direction

Figure 5.1: *Sketch of the reservoir condition flooding rig used in the SACS Task 3.2. flooding and geochemical reaction experiments.*



The preserved plugs were used for the CO₂ flooding experiments, but they were fairly short (L~7-8 cm) and to measure a precise permeability required a high flow rate to generate a measurable differential pressure. This of course amplified the fines problem, and GEUS finally decided to produce a long core holder (L~50 cm) with a reduced sample diameter (D~2.5 cm) to measure precise permeabilities. The permeability data in table 5.3 have been measured using this long core holder.

5.4 Dynamic CO₂ flooding experiments

The experimental rig. Tubing and core holder was 316SS, rubber sleeves to confine the samples were hydrogenated Nitrile rubber. Flow rate and pressure was controlled by a PC driven HP pump (Quizix) with Hastelloy C-276 and SiC in the wetting parts. Interface piston cylinders was made from Ti and an internal volume of ~2 liters was sufficient for conducting the experiments without interrupting the flow. A drawing of the rig is shown in fig. 5.1. The CO₂ reaction experiments was performed under constant flow rate and at reservoir conditions, 37 °C and a pore pressure of 100 bar. Hydrostatic confining pressure was 162 bar. The fluid aliquots for chemical analysis was sampled in a pipette. The sampling caused a sudden flow of approx. 10 ml fluid through the sample under test. This later turned out to be a problem for the modelling of the experiments, and GEUS finally modified the rig with a by-pass loop the secure a constant flow even during sampling. This modification is shown in the rig drawing in fig. 5.1.

CO₂ flooding experiments. Two preserved plug samples taken from the frozen core have been run under the short term dynamic flooding programme performed at GEUS. Three experiments were carried out at reservoir temperature (37 °C) and lasted 14 days and 31 days respectively. The first flooding experiment which lasted 14 days was a blind run without CO₂ added to the formation brine. In the following experiments fresh CO₂ -saturated formation brine was flooded through the samples for periods of 14 and 31 days respectively. The brine flow rate was set at two different values to look for changes in reaction rate between CO₂ -saturated brine and the minerals of the Utsira sand. A number of reacted formation water samples were collected and sent to BGS for chemical analysis. Table 5.4 is an overview of the flooding and sampling scheme. Table 5.5 is a listing of the analytical results obtained. As appears Ca is the most reactive element – presumably due to dissolution of calcite shell fragments in the Utsira sand. Fig. 5.2 show the liquid throughput vs. time and the sampling events appear as small pulses on the time curve.

During the CO₂ reaction experiments the permeability should be logged. The applied low flow rate causes a very low differential pressure (< 0.1 bar) across the high permeability sand that makes the measured liquid permeabilities very uncertain. With the low flow rates and short core samples used during the CO₂ reaction experiments a simultaneous measurement of permeability is not possible. Solution/precipitation processes due to reaction may be recorded by weighing the sample before and after test. When chemical reaction is subtle, changes in weight due to solution/precipitation processes unfortunately are completely overruled by the fines migration problem.

5.5 Permeability conclusions

As pointed out earlier no evidence can be given that the preserved unconsolidated Utsira sand core received for analysis is undisturbed relative to the reservoir sand. It is observed that different sandpacks produces different permeability figures. Packing of the sand and fines migration is by far the most important phenomena affecting the measured permeability, even overshadowing the effect of confining pressure. After repeated testing of many samples it is fair to conclude that the gas and Klinkenberg corrected gas permeability for the tested Utsira sand core section is within the range 1.5-2.5 D. The liquid permeability is lower at 1-1.5 D, mainly due to fines migration. In the CO₂ reaction experiments Ca seems to be the most reactive element due to solution of carbonate shell fragments in the sand, but many experimental problems were encountered during this part of the study.

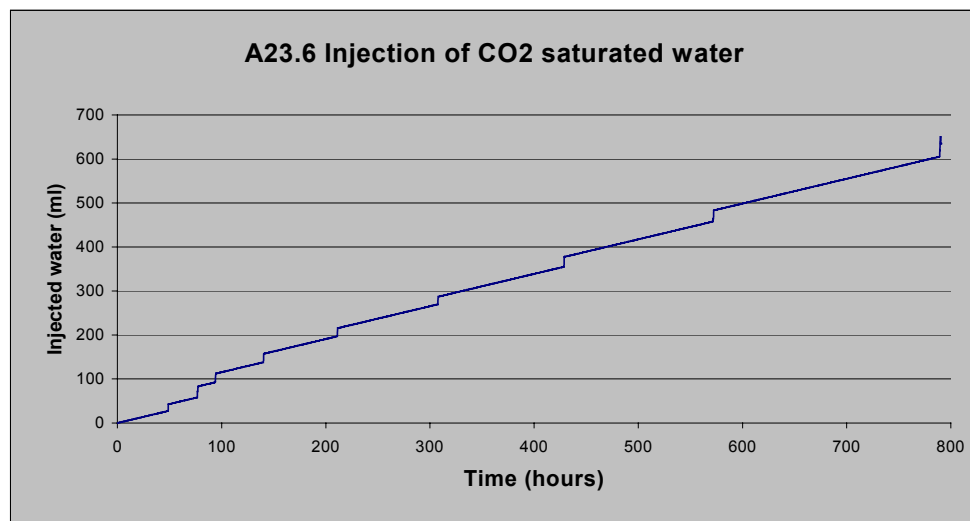
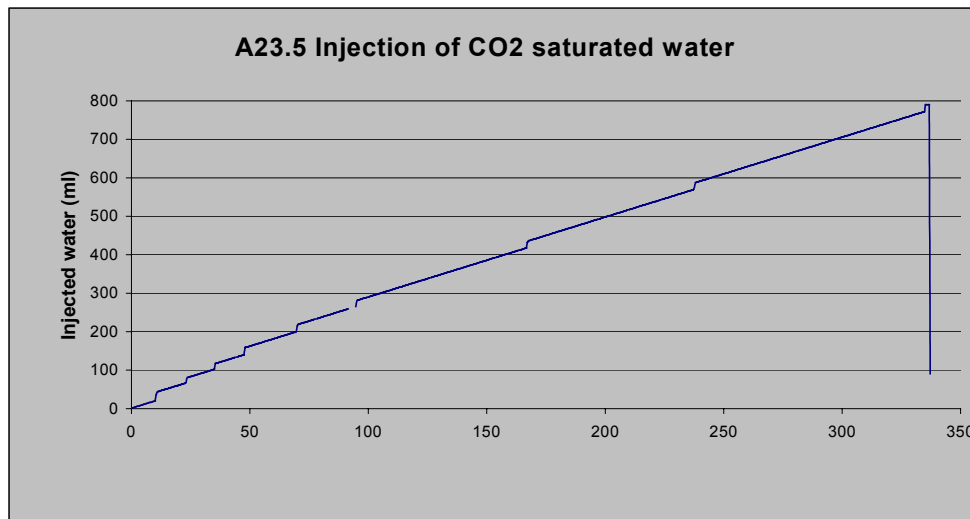
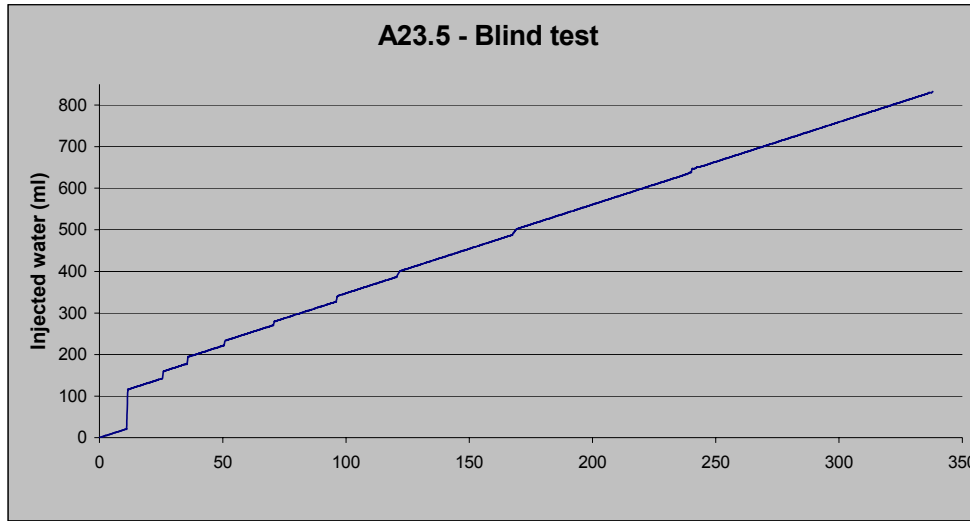
Table 5.4. Experiment plan for the short to medium term dynamic flooding experiments. Flow rates within a factor of 3 is tested, and the flow front velocity, applicable on a field scale as well, is given. Fluid samples of 10 ml volume are withdrawn from the experiment downstream line at the specified periods. The sum of the injected CO₂ – saturated formation brine is given at a nominal scale; the actual volume is listed in table 5.5.

Nom. plug data:	L, [cm]	D, [cm]	BV, [cc]	Ø, [%]	PV, [cc]	Reservoir conditions							T=37 °C
	7.5	3.8	85.1	38	32.3	Flooding schedule: 3 and 10 PV's per week							
Flow rate: 10 PV/week ~ 320 ml/week ~ 45.7 ml/d ~ 1.90 ml/h					Front velocity: 11 cm/d ~0.45 cm/h					Sample no.: A23.5		KI ~ 950 mD	
Blind run													
Fluid sampling point:	Day 0	Day 0+12h	Day 1	Day 1+12h	Day 2+6h	Day 3	Day 4	Day 5	Day 7	Day 10	Day 14	Total [ml]	
Fluid sample 1 ID													
Fluid sample 2 ID													
Σ fluid injected	0	23+10	56+10	89+10	133+10	177+10	233+10	289+10	390+10	537+10	730+10	740	
Flow rate: 10 PV/week ~ 320 ml/week ~ 45.7 ml/d ~ 1.90 ml/h					Front velocity: 11 cm/d ~0.45 cm/h					Sample no.: A23.5		KI ~ 950 mD	
Reaction run													
Fluid sampling point:	Day 0	Day 0+12h	Day 1	Day 1+12h	Day 2+6h	Day 3	Day 4	Day 5	Day 7	Day 10	Day 14	Total [ml]	
Fluid sample 1 ID													
Fluid sample 2 ID													
Σ fluid injected	0	23+10	56+10	89+10	133+10	177+10	233+10	289+10	390+10	537+10	730+10	740	
Flow rate: 3 PV/week ~ 96 ml/week ~ 13.7 ml/d ~ 0.57 ml/h					Front velocity: 3.2 cm/d ~0.134 cm/h					Sample no.: A23.6		KI = 990 mD	
Reaction run													
Fluid sampling point:	Day 0	Day 1	Day 2	Day 3	Day 4	Day 6	Day 9	Day 13	Day 18	Day 24	Day 31	Total [ml]	
Fluid sample 1 ID													
Fluid sample 2 ID													
Σ fluid injected	0	13.7+10	37+10	61+10	85+10	122+10	173+10	238+10	317+10	409+10	515+10	525	

Table 5.5. Chemical data measured at BGS analytical facility on small liquid fractions withdrawn from short term dynamic flooding experiments performed at GEUS. Data are shown from one blind run and 2 runs where Utsira sand was reacted with fresh CO₂-saturated formation brine injected into the upstream end of the sample at reservoir temperature (37 °C). Runtime, brine injected as well as brine volume corrected for withdrawal of liquid samples are given in the table.

LIMS Code	Sample Code	Ca mg/l	Mg mg/l	Na mg/l	K mg/l	Total P mg/l	Si mg/l	Ba mg/l	Sr mg/l	Mn mg/l	Total Fe mg/l	Al mg/l	Li mg/l	Run type	Time	Recorded brine production	Corrected brine production
06642-00001	Distilled water	0.098	<0.010	<0.350	<0.500	0.016	<0.075	<0.002	<0.002	0.003	<0.010	<0.100	<0.025		hours		
06642-00002	Synthetic brine	172	568	9450	233	<0.100	0.389	0.311	5.11	0.046	0.371	<1.00	<0.250			ml	ml
06642-00003	5/14.02A	256	612	10957	293	<0.100	2.95	0.642	7.60	2.61	0.389	<1.00	<0.250	blind run	0.0	0.0	0.0
06642-00004	5/14.02B	237	627	10925	302	<0.100	1.53	0.563	7.33	0.536	0.394	<1.00	<0.250	-	11.0	21.0	20.9
06642-00005	5/15.02A	230	598	10600	258	<0.100	3.19	0.676	7.07	0.630	0.375	<1.00	<0.250	-	25.5	142.6	48.5
06642-00006	5/15.02B	243	609	10574	260	<0.100	3.20	0.696	7.57	0.468	0.387	<1.00	<0.250	-	35.5	178.2	67.5
06642-00007	5/16.02	167	559	10106	235	<0.100	3.13	0.557	5.84	0.394	0.365	<1.00	<0.250	-	50.5	221.7	96.0
06642-00008	5/17.02	165	567	10652	236	<0.100	2.93	0.563	5.72	0.391	0.371	<1.00	<0.250	-	70.5	270.6	134.0
06642-00009	5/18.02	186	583	9828	242	<0.100	2.57	0.566	5.67	0.458	0.390	<1.00	<0.250	-	96.0	327.2	182.4
06642-00010	5/19.02	241	647	10572	269	<0.100	2.74	0.709	7.37	0.444	0.403	<1.00	<0.250	-	120.5	386.6	229.0
06642-00011	5/21.02	180	559	9634	236	<0.100	2.21	0.568	5.36	0.634	0.365	<1.00	<0.250	-	167.0	488.2	317.3
06642-00012	5/24.02	227	600	10387	254	<0.100	2.19	0.695	7.04	0.847	0.378	<1.00	<0.250	-	238.5	634.6	453.2
06642-00013	5/28.02	202	607	10712	258	<0.100	1.85	0.672	6.05	1.27	0.369	<1.00	<0.250	-	335.5	828.2	637.5
06642-00014	5/06.03A	185	560	10553	231	<0.100	2.95	0.725	6.35	1.28	0.360	<1.00	<0.250	blind run	0.0	0.0	0.0
06642-00015	5/06.03B	273	575	9734	251	<0.100	7.87	0.322	3.59	3.16	0.363	<1.00	<0.250	CO2 run	10.0	20.0	19.0
06642-00016	5/07.03A	174	640	10990	289	<0.100	1.77	0.174	1.18	0.850	0.408	<1.00	<0.250	-	23.0	67.2	43.7
06642-00017	5/07.03B	176	630	10301	270	<0.100	1.04	0.152	1.15	0.433	0.402	<1.00	<0.250	-	35.0	102.3	66.5
06642-00018	5/08.03	492	675	10415	286	<0.100	3.91	0.253	4.43	1.25	0.409	<1.00	<0.250	-	47.5	140.0	90.3
06642-00019	5/09.03	444	629	10794	264	<0.100	3.09	0.221	4.13	0.993	0.394	<1.00	<0.250	-	69.5	200.0	132.1
06642-00020	5/10.03	401	630	10761	265	<0.100	2.37	0.147	3.53	1.05	0.396	<1.00	<0.250	-	94.5	265.1	179.6
06642-00021	5/13.03	493	593	10746	244	<0.100	2.90	0.203	5.25	1.21	0.391	<1.00	<0.250	-	166.5	416.4	316.4
06642-00022	5/16.03	536	578	10853	242	<0.100	3.12	0.155	5.59	1.09	0.365	<1.00	<0.250	-	237.0	569.4	450.3
06642-00023	5/20.03	823	629	10557	259	<0.100	2.72	0.115	7.41	1.47	0.423	<1.00	<0.250	-	334.5	771.2	635.6
06642-00024	6/19.04	282	581	9723	261	<0.100	4.12	0.544	6.05	1.88	0.376	<1.00	<0.250	blind run	0.0	0.0	0.0
06642-00025	6/21.04	56.6	624	11032	302	<0.100	4.44	0.106	0.689	2.60	0.392	<1.00	<0.250	CO2 run	48.5	27.3	27.6
06642-00026	6/22.04	214	570	10291	267	<0.100	2.56	0.239	2.04	5.96	0.378	<1.00	<0.250	-	76.5	58.1	43.6
06642-00027	6/23.04	174	578	10311	259	<0.100	0.766	0.189	1.62	1.18	0.374	<1.00	<0.250	-	94.0	94.0	53.6
06642-00028	6/25.04	317	568	10650	246	<0.100	3.36	0.201	3.68	2.40	0.366	<1.00	<0.250	-	140.0	138.1	79.8
06642-00029	6/28.04	176	535	9795	230	<0.100	0.601	0.170	1.55	0.253	0.365	<1.00	<0.250	-	211.0	197.1	120.3
06642-00030	6/02.05	234	569	10896	237	<0.100	1.09	0.201	1.91	1.11	0.351	<1.00	<0.250	-	307.5	269.6	175.3
06642-00031	6/07.05	206	561	10190	235	<0.100	1.42	0.158	1.63	0.419	0.357	<1.00	<0.250	-	428.5	355.0	244.2
06642-00032	6/22.05	350	590	10740	246	<0.100	3.55	0.137	3.40	0.714	0.384	<1.00	<0.250	-	571.5	457.8	325.8
06642-00033	6/13.05	380	502	10884	211	<0.100	3.28	0.154	4.14	2.40	0.357	<1.00	<0.250	-	789.0	605.2	449.7

Fig. 5.2. Injection vs. time curves for the three experiments. A step on the curve represents withdrawal of a fluid sample of approx. 10 ml from the downstream side of the sample – a volume which is immediately replaced, at the upstream side, by the computer controlled pumping system to keep up the system pressure.



6 Analytical Methods

The following is a short description of the methods used by GEUS Core Laboratory. For a more detailed description of methods, instrumentation and principles of calculation the reader is referred to API recommended practice for core analysis procedure (API RP 40, 1998).

6.1 Conventional cleaning and drying

The plugs are drilled and trimmed to a size as required by the client. The samples are then placed in a Soxhlet extractor, which continuously soaks and washes the samples with methanol. This process removes water and dissolves salt precipitated in the pore space of the rock. Extraction is terminated when no chloride ions are present in the methanol. Samples containing hydrocarbons are then cleaned in toluene until a clear solution is obtained. Samples are vacuum dried at 90 °C or 110 °C, or they are humidity dried at 60 °C and 40% relative humidity until constant weight occurs, depending on the requirements of the client.

6.2 Gas permeability (GEUS steady state instrument)

The plug is mounted in a Hassler core holder, and a confining pressure of 400 psi (or specified by the client) applied to the sleeve. The specific permeability to gas is measured by flowing nitrogen gas through a plug of known dimensions at differential pressures between 0 and 1 bar. No back pressure is applied. The readings of the digital gas permeameter are checked regularly by routine measurement of permeable steel reference plugs (Core Laboratories™ gas permeability reference plug set).

6.3 Klinkenberg permeability (GEUS steady state instrument)

The Klinkenberg corrected gas permeability, sometimes termed the equivalent liquid permeability, is calculated from gas permeability measurements performed at 3 different mean pressures in the plug sample.

The plug is mounted in a Hassler core holder, and a confining pressure of 400 psi (or specified by the client) is applied to the sleeve. Nitrogen gas pressures of 3, 5 and 8 atm. (abs.) are applied at the upstream end of the plug, and the downstream pressure is regulated until a suitable flow is obtained. The differential pressure is kept approx. constant in order to maintain a similar flow regime during the 3 measurements. When a steady state is reached, the upstream pressure, the differential pressure across the plug and the flow reading is recorded. A linear regression of permeability on inverse mean pressure is performed for the 3 measurements, and the intercept on the permeability axis is the Klinkenberg corrected gas permeability. To ensure compatibility with plug data which do not include Klinkenberg corrected gas permeability, a permeability value pertaining to a mean pressure of 1.5 atm. (abs) is calculated from the Klinkenberg regression coefficients. This value is reported as "1.5 P-M permeability" in the core analysis tabulation, and should be comparable to the conventional gas permeability which is measured at the same mean pressure.

Klinkenberg corrected gas permeabilities are only reported down to approx. 0.1 mD on normal routine terms. However, on request measurements can be carried out to a lower limit of 0.01 mD. The performance of the digital gas permeameter is checked regularly by routine measurements of permeable steel reference plugs (Core Laboratories™ gas permeability reference plug set).

6.4 Liquid permeability

The liquid permeability is measured by flowing brine through the sample at a suitable differential pressure. The measurement is performed at room or reservoir temperature with or without back pressure applied. The confining pressure is applied according to the requirements of the client. The measurement continues until the permeability is approximately constant with time. The reported liquid permeability is the mean value of several determinations performed over a period of minutes to a few hours, depending on the permeability of the sample.

6.5 He-porosity and grain density

The porosity is measured on cleaned and dried samples. The porosity is determined by subtraction of the measured grain volume and the measured bulk volume. The Helium technique, employing Boyle's Law, is used for grain volume determination, applying a double chambered Helium porosimeter with digital readout, whereas bulk volume is measured by submersion of the plug in a mercury bath using Archimedes principle. Grain density is calculated from the grain volume measurement and the weight of the cleaned and dried sample. The Helium porosimeter is calibrated using a set

of steel plugs (Core Laboratories™ volume reference plug set) before the measurement of plug samples are initiated. By exchanging the sample cup with a core holder, the instrument is converted to a single cell porosimeter that allows a determination of the porosity of unconsolidated samples.

6.6 Archimedes porosity

Samples that are saturated to 100% with a liquid can have their bulk volume determined by Archimedes test, i.e. by submersion in a jar containing the saturating liquid and weighing of the buoyancy. If the sample grain density is known (e.g. from a He-porosity measurement) or can be estimated with good precision, the sample pore volume and porosity can be calculated.

6.7 Reduced porosity by overburden pressure.

The initial porosity is determined at room conditions or from an Archimedes test applied to the fully brine saturated plug sample. During testing the sample pore volume decreases as overburden increases. This is observed as an amount of liquid expelled from the sample and constantly monitored using an electronic Mettler balance connected to a PC. The final reading is taken when a stable level has been obtained on the balance. The porosity reduction is calculated as the relative decrease in the initial porosity:

$$\phi_i = \frac{V_{pi}}{V_{bi}}$$

$$\phi_{i+\Delta p} = \frac{V_{pi} - \Delta V_p}{V_{bi} - \Delta V_p}$$

The porosity reduction is then given as:

$$\frac{\phi_{i+\Delta p}}{\phi_i} \cdot 100\% = \frac{V_{pi} - \Delta V_p}{V_{bi} - \Delta V_p} \cdot \frac{V_{bi}}{V_{pi}} \cdot 100\%$$

Where ϕ_i = Initial porosity
 V_{pi} = Initial pore volume
 V_{bi} = Initial bulk volume
 $\phi_{i+\Delta p}$ = New porosity induced by a certain change Δp in overburden pressure
 ΔV_p = Change in pore volume due to the change Δp in overburden pressure

The initial change in the pore volume (PV_0) that occurs from room conditions to the lowest overburden pressure applied in the study is extrapolated from a liquid production curve (produced liquid vs net overburden pressure).

The produced liquid was measured at 10, 30, 50, 70 and 100 bar confining pressure. From these measurements the liquid production curve was fitted. The slope of the regression curve at 10 bar was extrapolated to 0 bar, to determine the initial change in the pore volume PV_0 .

6.8 Pore volume compressibility

The pore volume compressibility is calculated from the data recorded during the porosity reduction experiment as follows:

$$C_p = \frac{1}{V_p} \cdot \frac{dV_p}{dp_{eff}}$$

where: C_p = Pore volume compressibility [vol/vol*psi]
 V_p = Sample pore volume at a certain net overburden pressure (NOP)
 dV_p = Incremental change in pore volume resulting from an incremental change in NOP
 dp_{eff} = Incremental change in NOP

The relationship dV_p/dp_{eff} is obtained by graphical differentiation of the liquid production curve. Both the incremental change of pore volume and the pore volume compressibility is calculated from the liquid production curve.

6.9 Precision of analytical data

The table below gives the precision (= reproducibility) at the 68% level of confidence (+/- 1 standard deviation) for routine core analysis measurements performed at GEUS Core Laboratory.

Measurement	Range, mD	Precision
Grain density		0.003 g/cc
Porosity		0.1 porosity-%
Permeability: (Klinkenberg)	0.01-0.1	15%
	0.1-1	10%
	> 1	4%
Permeability: (Conventional)	0.001-0.01	25%
	0.01-0.1	15%
	> 0.1	4%

6.10 Nomenclature

L	– sample length [cm]
D	– sample diameter [cm]
BV	– bulk volume [cc]
PV	– pore volume [cc]
GV	– grain volume [cc]
DW	– dry weight [g]
Ø	– porosity [pct. or fraction]
K	– permeability [mD or D]
S _{BET}	– specific surface area by Nitrogen absorption [m ² /g]
CEC	– cation exchange capacity [meq. Na ⁺ /100 g]
d	– day(s)
h	– hour(s)
TVD _{ss}	– total vertical depth, sub sea [m]

7 References

SACS 0: Saline Aquifer CO₂ Storage – S.A.C.S., Phase 0.
Ulrik Gregersen (ed.), 1998.

SACS I: Final Technical Report of project 'Saline Aquifer CO₂ Storage'. Work Area 1: GEOLOGY
Peter Zweigel (ed.), 2000.

Priisholm, S., Nielsen, B.L. & Haslund, O.: "Fines migration, blocking and clay swelling of potential geothermal sandstone reservoirs, Denmark. SPE Formation Evaluation, June 1987.